AIChE

Simulation of Particle Migration in Free-Surface Flows

Kyung Hoon Min and Chongyoup Kim
Dept. of Chemical and Biological Engineering, Korea University, Anam dong, Sungbuk-ku, Seoul 136-713, Korea

DOI 10.1002/aic.12145
Published online February 22, 2010 in Wiley Online Library (wileyonlinelibrary.com).

The migration of particles in free surface flows using the diffusive flux model was investigated. As the free-surface flows, a planar jet flow and a slot coating flow were chosen. The suspension was assumed to be a Newtonian fluid with a particle concentration dependent viscosity. The governing equations were solved numerically by the finite volume method, and the free-surface problem was handled by the volume of the fraction model. The result shows that even though the velocity profile is fully developed and becomes flat, the particle distribution never reaches the uniform distribution for both of the cases. It is also shown that the die swell of the free jet is reduced compared to the Newtonian fluid and when the particle loading is 0.5, die contraction is observed. The change in die swell characteristics is purely due to particle migration since the suspension model does not show normal stress differences. © 2010 American Institute of Chemical Engineers *AIChE J,* 56: 2539–2550, 2010

Keywords: particle migration, free jet, slot coating, diffusive flux model, die contraction

Introduction

Since the pioneering report on the migration of spherical particles in inhomogeneous flows by Leighton and Acrivos,[1] there have been numerous theoretical and experimental studies on the migration of particles in various geometries. However, most of the studies on particle migration have been limited to the flows inside solid boundaries, and there have been only a few reports on the free-surface flow of suspension. It appears that Husband et al.[2] first reported the migration of particles in a free-surface flow. They performed experimental studies on the flow of bimodal suspensions along an inclined surface and found that large particles moved toward the free surface. Tirumkudulu et al.[3,4] considered the partially filled horizontal cylinder rotating in its axis showing that there was the segregation of particles to form band structures along the axis and subsequent studies by Timberlake and Morris[5] showed that the particle migration model could explain the instability phenomena. Recently Timberlake and Morris[6] performed experimental researches on the gravity driven free-surface flow of a suspension of neutrally buoyant spherical particles down an inclined plane, Singh et al.[7] considered a gravity-driven inclined channel flow and Loimer et al.[8] studied the free surface in the vorticity direction formed by the two belts to generate the plane Couette flow. The studies by Timberlake and Morris[6], Singh et al.[7] and Loimer et al.[8] observed the free-surface structure of many length scales, both larger and smaller than the particle size despite the fundamental difference in flow geometry and flow pattern. However, no study has yet precisely measured or estimated the particle concentration profile near the free surface and the free-surface flow of suspension is far from being fully understood. It is evident that we need more studies to understand the free-surface flow of suspensions both experimentally and theoretically. Especially we need more studies on the distribution of particle concentration and its relation with the velocity profile considering the practical application in many industrial processes where particle migration is an important issue.

In the electronic industry, many different kinds of slurries are processed.[9–11] Some of the processes have free surfaces and some free-surface flows of suspensions are similar to the free jet flow. In the generation of an inkjet drop, for example, a fluid element with suspended particles is ejected from

Correspondence concerning this article should be addressed to C. Kim at cykim@grtrkr.korea.ac.kr.

the nozzle and forms a long liquid column behind the spherical head. During the flow through the piezoelectric nozzle, the particles may migrate to the center due to the nonhomogeneous flow inside the nozzle and then they will redistribute during the formation of a ligament and the subsequent contraction of the ligament outside the nozzle. Depending on the uniformity of particle distribution inside the suspension drop, the impinging characteristics and the final drying pattern of the impinged suspension will vary. In the dispensing of fluorescent suspensions to fill in the trough of less than 0.5 mm in PDP (plasma display panel) manufacturing industries, inside the nozzle, almost the same physical process occurs. The liquid jet emerged from the nozzle travels for a short distance before it reaches the trough. During the travel of the jet particles segregated inside the nozzle have to be redistributed for a better performance. Suspensions of various levels of particle-loadings are also used in many coating processes. For example, both of the electrodes of lithium-ion batteries are manufactured by the slot coating processes of the slurries. To improve the quality of coating products, it is very important to keep the particle distribution uniform throughout the flow paths.

Keeping in mind the fact that the aforementioned processes require the understanding of the particle distribution and velocity profile within the flow domain, in this study, we consider two different classes of the migration problems with free surfaces. The first one is the planar jet problem. In this case, the fully developed downstream velocity is not known *a priori*, and the downstream velocity and the thickness of the jet have to be determined as parts of the solution. The second one is the slot coating problem. In this case we specify the flow rate and web velocity as the part of the problem, hence, the downstream velocity and the position of the free surface are known *a priori*.

Until now, many approaches that simulate particle migration in suspension have been attempted and they can be classified as the ''diffusive flux model'' (Phillips et al.[12]) in which particle migration is driven by the shear rate gradient and the ''suspension balance model'' (Jenkins and McTigue,[13] Nott and Brady,[14] Morris and Boulay,[15] and Miller and Morris[16]) in which particle migration is driven by the gradient in the normal stress differences. As part of the suspension balance model Nott and Brady[14] introduced a novel concept of ''suspension temperature'' which is the fluctuation of the particle kinetic energy caused by the collisions among particles. In the case of channel flow the Stokesian simulations were in good agreement with the model predictions based on the suspension temperature. Both of the models have their own merits. The diffusive flux model is more phenomenological; the suspension balance model gives better insight on the fundamental physics of the problem. Especially the singularity at the channel center does not appear in the case of Nott and Brady's model. It is not intended to compare the difference between these models extensively in this research. Rather we consider whether the diffusive flux model will be appropriate in understanding the migration phenomena. The concept of the diffusive flux model was first introduced by Leighton and Acrivos[1] in their seminal article on particle migration. They extracted the scaling laws in the particle migration and gave the concept of the diffusion by the particle collision. Phillips et al.[12] proposed the diffusive flux model considering the migration phenomena due to gradients in shear rate and viscosity. They successfully fitted their NMRI data on the Couette and Poiseuille flows to the model calculations at the steady and transient states. Subia et al.[17] performed the simulation using the model of Phillips et al.[12] and compared with their NMRI experiments on the piston flow and eccentric cylinder flow. They showed that the shear-induced migration model was robust at capturing the essential features in two- and three-dimensional problems. Recently Kim et al.[18] successfully applied the diffusive flux model to the migration of spherical particles suspended in the Newtonian fluid under the torsional flows. By incorporating the curvature induced migration mechanism by Krishnan et al.[19] to the original model of Phillips et al.[12] they predicted the experimental observations of the particle migration in the transient state at least semiquantitatively including the development of the shock in particle concentration profiles. Shapley et al.[20] critically compared the predictions of several suspension temperature models of particle migration to the experimental measurements in a concentrated suspension of noncolloidal spheres. They observed that the observed macroscopic shear rate and particle-volume fraction profiles were fairly well matched at moderate bulk-particle fractions, but different from each other at high-particle concentrations. They also observed that the predictions of the suspension temperature and diffusive flux models were strikingly similar for the narrow gap Couette flow, and concluded that the suspension temperature models did not appear to have a significant advantage over the diffusive flux models. Another important point is the suspension temperature prediction by the suspension balance model. The suspension temperatures predicted by the suspension balance model (Nott and Brady[14]) are not consistent with the experimental observation, and there is two-orders of magnitude difference in the flow direction, and the suspension temperatures are not isotropic (Lyon and Leal[21]) as assumed in the suspension balance model. Therefore, the suspension balance model based on the suspension temperature cannot predict properly the normal stress difference which may have a significant role in die swell of free-surface flow. To account for the die swell the suspension balance model based on the normal stress should be the best choice in principle. However, until now the normal stress driven model cannot be considered sufficiently accurate. The migration predicted by Miller and Morris[16] shows a difference between the model prediction and experimental observation. Another fact is that even without the normal stress difference the change in die swell characteristics can be still predicted in the case of the diffusive flux model. This point will be considered later in this article.

Considering the economy of the calculation and the accuracy of the result, the diffusive flux model could be a better choice in the simulation of the particle migration. Therefore, in this research, we applied the diffusive flux model by Phillips et al.[12] to the migration problem with free surfaces. In the next section, we formulate the problems. Then we describe the numerical technique and the validation of the numerical method. Finally we describe the numerical result and discuss the meaning of our results.

Formulation of the problem

Let us consider semi-infinite two parallel plates with a gap distance d, as shown in Figure 1a. The plates are

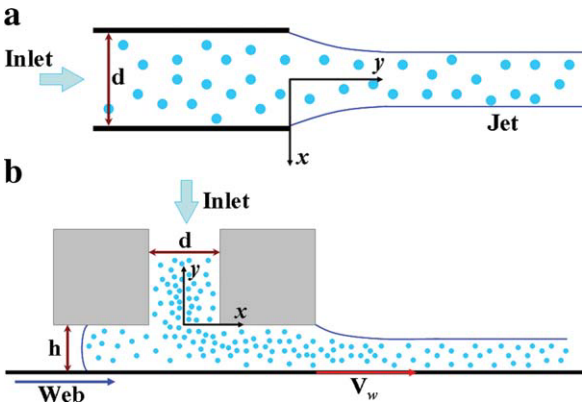

Figure 1. Geometries of the flows: (a) jet-flow system, and (b) slot coating flow system.

[Color figure can be viewed in the online issue, which is available at wileyonlinelibrary.com.]

extended in the y- and z-directions semi-infinitely and infinitely, respectively. A suspension with particle loading ϕ flows through the channel at a constant flow rate along the y-axis and comes out of the channel forming free surfaces. It is assumed that the temperature of the system is steady and uniform. The flow is steady from a macroscopic point of view even though the particles interact with each other and the wall during flow. Particles suspended in the Newtonian fluid are neutrally buoyant, and the radii of the particles are the same at a. The particle size is large enough to neglect the Brownian motion of the particle, say larger than 1 μm, but small enough to regard the suspension as a continuum and to neglect the wall effect. This is a necessary condition for net migration of particles since the Brownian motion will smooth out the concentration gradient developed by the migration. It is also assumed that there is no inertial effect due to particles since the Reynolds number based on particle diameter is sufficiently small. We consider two different cases for the downstream. First, we consider that there is no barrier at the exit of the channel. Then the flow becomes a 2-D jet problem. Second, we consider a slot coating system where a flat plate is placed perpendicular to the parallel plates and moving with a constant velocity v_w (web speed, See Figure 1b). In this case, each of the parallel plates has a wing of finite size that is parallel to the moving web. The gap distance between the wings and the moving web has about the same size as the gap distance d.

We assume that the particle migration can be expressed by the model by Phillips et al.[12] where particle migration occurs due to shear rate gradient and viscosity gradient. Phillips et al. deduced that the fluxes due to the nonuniform velocity and viscosity gradients are given as follows

$$N_c = -K_c a^2 (\phi \nabla(\dot{\gamma}\phi)) \tag{1}$$

$$N_\eta = -K_\eta \dot{\gamma} \phi^2 \left(\frac{a^2}{\eta}\right) \frac{d\eta}{d\phi} \nabla\phi, \tag{2}$$

where K_c and K_η are a constant, ϕ is the fraction of the particle, $\dot{\gamma}$ is shear rate, and a is the radius of particle. In this model it is postulated that the particle migration velocity of a test particle is proportional to the difference in the rate of collision, which is proportional to $a\nabla(\dot{\gamma}\phi)$ over a distance $O(a)$, and this collision gives rise to a displacement of $O(a)$. Here, it is also assumed that the collision frequency is proportional to both $\dot{\gamma}$ and ϕ, hence $\dot{\gamma}\phi$. This gives the flux due to the shear rate gradient. As there develops a concentration gradient due to shear rate gradient the viscosity changes accordingly. Over a distance $O(a)$, the fractional change in viscosity will be $a\frac{\nabla\eta}{\eta}$. If it is postulated that each interaction causes a displacement of $O(a)$, considering that the collision frequency is proportional to $\dot{\gamma}\phi$ the migration velocity due to the viscosity gradient will be proportional to $(\dot{\gamma}\phi)(a^2/\eta)\nabla\eta$. The migration fluxes can be obtained by multiplying the migration velocities with particle-volume fraction as given in Eqs. 1 and 2. The total flux of particle can be obtained by the sum of the fluxes due to the shear-induced migration and viscosity-induced migration (the sum of Eqs. 1 and 2)

$$N_t = N_c + N_\eta \tag{3}$$

The governing equations are the continuity and momentum equations for fluid flow and diffusion equation for the particle distribution

$$\frac{\partial \rho}{\partial t} + \nabla \cdot (\rho \vec{\mathbf{v}}) = 0 \tag{4}$$

$$\frac{\partial \rho \vec{\mathbf{v}}}{\partial t} + \rho \vec{\mathbf{v}} \cdot \nabla \vec{\mathbf{v}} = -\nabla p + \nabla \cdot (\bar{\bar{\tau}}) + \rho \vec{\mathbf{g}} + \vec{\mathbf{F}} \tag{5}$$

$$\frac{\partial \phi}{\partial t} + \vec{\mathbf{v}} \cdot \nabla \phi = -\nabla \cdot (N_t) \tag{6}$$

where ρ is the density of suspension, $\vec{\mathbf{v}}$ is velocity vector, p is pressure, $\bar{\bar{\tau}}$ is stress tensor, $\vec{\mathbf{g}}$ is the gravitational acceleration, and $\vec{\mathbf{F}}$ denotes body forces. It is assumed that the velocity of particle is the same as the velocity of the liquid. The stress tensor $\bar{\bar{\tau}}$ is expressed by a Newtonian fluid with concentration dependent viscosity, thus

$$\bar{\bar{\tau}} = \eta(\phi)\bar{\bar{\dot{\gamma}}} \quad (\bar{\bar{\dot{\gamma}}} = \nabla \vec{\mathbf{v}} + \nabla \vec{\mathbf{v}}^T) \tag{7}$$

Here Krieger's model is used for the viscosity model

$$\eta = \eta_s (1 - \phi/\phi_m)^{-1.82} \tag{8}$$

In the aforementioned equation η is the viscosity of suspension, η_s is the viscosity of the dispersing medium, and ϕ_m is the maximum packing fraction of particle and is 0.68 for hard spheres.

For the momentum equation, no-slip condition is applied at the solid wall and normal and tangential force conditions are applied at the free surfaces, thus

$$\mathbf{v}_s = 0 \quad \text{(at the solid boundary)} \tag{9}$$

$$\mathbf{n} \cdot \bar{\bar{\tau}} \cdot \mathbf{n} = 2H\sigma = -\sigma \nabla \cdot \mathbf{n} \quad \text{(at the fluid boundary)} \tag{10}$$

$$\mathbf{t} \cdot \bar{\bar{\tau}} \cdot \mathbf{n} = 0 \quad \text{(at the fluid boundary)} \tag{11}$$

For particle migration equation, no-flux condition is applied at both of the walls and free surfaces

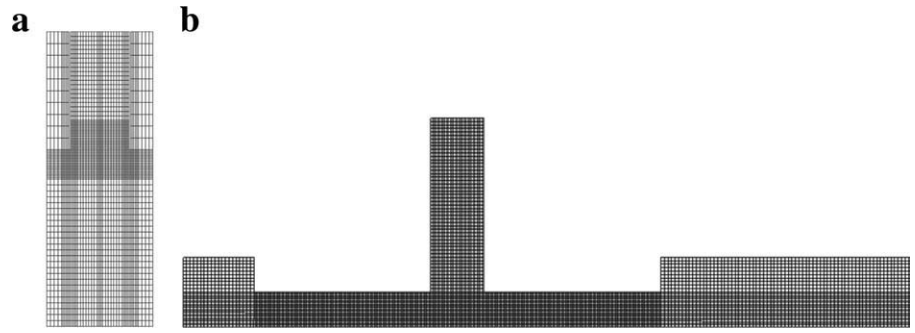

Figure 2. Meshes for the FVM (a) jet flow, and (b) slot coating flow.

$$\mathbf{n} \cdot \left(K_c \phi \nabla(\dot{\gamma}\phi) + K_\eta \dot{\gamma} \phi^2 \frac{1}{\eta} \frac{d\eta}{d\phi} \nabla \phi \right) = 0 \tag{12}$$

In Eqs. 10, 11 and 12, **n** is the surface normal, and **t** is the tangential vector to the surface. Also H and σ denote the mean curvature and surface tension.

Numerical method

Rather than writing a homemade code, we used a commercial software package, Fluent™ based on the FVM (finite volume method). The FVM method has been successfully used by Fang and Phan-Thien[22] in the particle migration simulation. To handle the two-phase problems, we used the volume of fraction (VOF) model of Fluent.

To solve the particle migration equation which is not in the standard form of the diffusion equation for Fluent, we devised a technique by using the user-defined functions of Fluent. We set the sum of the righthand-side term of Eq. 6, and the Brownian diffusion term in the standard form of the diffusion equation (Eq. 13) to be the source term (S, Eq. 14) of the diffusion equation to fit the governing equations to the standard format of the Fluent software, thus

$$\frac{\partial \phi}{\partial t} + \vec{\mathbf{v}} \cdot \nabla \phi = -\nabla \cdot (-D \nabla \phi) + S \tag{13}$$

where

$$S = -\nabla \cdot \left(-K_c \phi \nabla(\dot{\gamma}\phi) - K_\eta \dot{\gamma} \phi^2 \frac{1}{\eta} \frac{d\eta}{d\phi} \nabla \phi \right) + \nabla \cdot (-D \nabla \phi) \tag{14}$$

In solving the governing equations we did not nondimensionalize the equations as the Fluent software does not require such a process.

In Figure 2, the FVM meshes for the jet and coating flows are shown. In the case of the jet flow the total numbers of nodes and cells were 3,614 and 3,460, respectively. In the case of coating flow, 9,211 nodes and 8,800 cells were used. Even though only the steady flow was concerned, the problems were formulated in the transient state and the time marching technique of the first-order backward implicit method was used. However, the transient solution was not considered since the initial condition imposed here was chosen so that the convergence was reached as fast as possible. Actually we used the steady-state solution of the previous problem as the initial condition for the next problem when the parametric studies were performed. The time step was determined so that we could obtain the converged solutions while keeping the accuracy, and these values were 10^{-5} and 10^{-6} s for the jet and coating flows, respectively.

To validate the numerical code, we performed calculations for the parallel plate system and compared with the semianalytic, implicit solution obtained by solving the 1-D problem as described in Phillips et al.[12] and Kim,[23] and given as follows

$$\frac{\phi}{\phi_w} = \left(\frac{1}{\xi - 1} \right) \left(\frac{1 - \phi/\phi_m}{1 - \phi_w/\phi_m} \right)^{-1.82} \tag{15}$$

$$\int_{-1/2}^{1/2} \phi(\xi) d\xi = \phi_0 \tag{16}$$

$$\frac{\dot{\gamma}}{\dot{\gamma}_w} = (\xi - 1) \left(\frac{1 - \phi/\phi_m}{1 - \phi_w/\phi_m} \right)^{-1.82} \tag{17}$$

In the aforementioned equations, subscript w denotes wall, and $\xi = x/d$ is the dimensionless coordinate across the channel. In Figure 3, we plotted the particle-concentration distributions and velocity profiles obtained by two different methods. In this case, for the economy of calculation we assumed that, at the inlet of the geometry, the particle distribution is the same as the analytical result for parallel plates system. The numerical solution catches the important features of particle migration such as the migration to the low-shear region and velocity blunting, and the agreement is excellent except the case of particle-concentration distribution at the line of symmetry. This discrepancy occurs because the Phillips et al.'s model has a singularity where the shear rate vanishes. The numerical solution cannot accommodate such singularity and the solution has a rounded profile. The same phenomenon was also observed in the finite element solution by Zhang and Acrivos.[24] Experimentally, Koh et al.[25] reported the smooth profile at the center of the channel. However, this is caused by the finite size of the particle and was analyzed by Han et al.[26] Our problem is basically a numerical artifact and the numerical solution can be made as closely as possible to the analytic solution by using extremely small elements in the neighborhood of the mathematical singularity. However, it

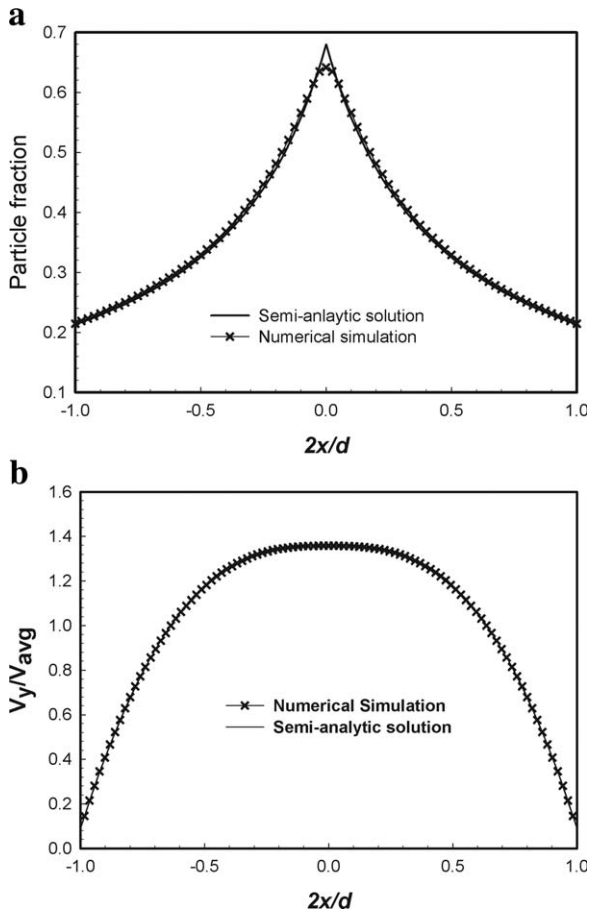

Figure 3. Particle distribution and velocity profile of the slit flow.

The particle loading is 0.5. The ratio of the gap size and the particle diameter is 40. The Reynolds number based on the gap distance and the viscosity of the well-mixed suspension is 3.56.

would not give any significantly better solution while the computation time increases formidably. Therefore, we regarded that the numerical code be validated and decided to use the current meshes for further calculations.

Result

Two-dimensional jet flow

We investigated the migration of particles in the jet flow first, because the jet flow bears many important features of the most of free-surface flows while keeping simplicity. In Figure 4, we show the particle concentration map at the steady state for the parameter set shown in Table 1. Since the purpose of the jet flow is to understand the qualitative nature of the migration in free-surface flows, the data set has been chosen so that the migration process can be easily demonstrated while keeping the basic assumptions of Phillips et al.'s model. We used 0.41 and 0.62 for K_c and K_η as suggested by Phillips et al.[12] In Figure 5, we plotted the particle fraction and velocity profiles across the gap and jet before, at and after the exit ($y = -2d$, $-d/2$, 0, $d/2$, $3d/2$). The fully developed profile of the particle concentration inside the die

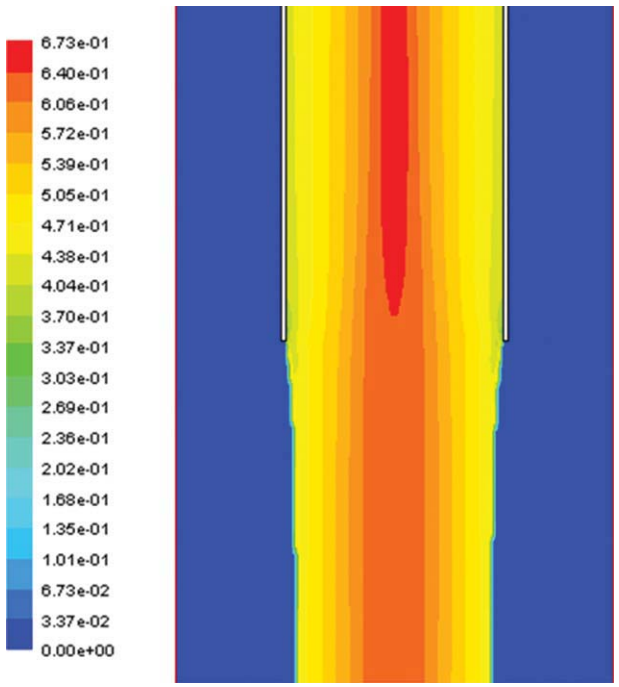

Figure 4. Particle distribution map of the jet flow.

The simulation condition is given in Table 1. [Color figure can be viewed in the online issue, which is available at wileyonlinelibrary.com.]

begins to be disturbed before the exit to the air. The exit length is approximately the same as one gap distance between two parallel plates. This result is much the same as the case of Newtonian fluid flowing through a circular die,[27] where the redistribution of axial velocity occurs after flowing about one radius of the die. The velocity and concentration profiles become fully developed after flowing by one gap distance. However, the fully developed distribution of particles is not uniform. The distribution is close to the upstream particle distribution profile before disturbed by the discharge to the air even though the velocity profile is fully developed and flat. The nonuniform particle distribution is the consequence of the fact that particle migration is a slow process compared to the momentum transport (In this case $D_{\text{hydrodynamic}}/v \approx \rho\dot{\gamma}a^2/\eta \approx 0.0025$). The length of flow to travel to reach the fully developed state requires an order of d^3/a^2.[14] In this research this is 1,600 times the gap distance. Since there is no gradient in shear rate in the jet with the flat velocity profile there is no particle migration. Unless fully mixed just before the die exit, the particle distribution

Table 1. Numerical Parameters for the Jet Flow Calculations

Gap size of the slot (d)	4 mm
Average inlet velocity	1 m/s
Contact angle	30°
Surface tension (σ)	0.05 N/m
Liquid viscosity	0.1 Pa.s
Liquid density	1000 kg/m^3
Particle size (a)	100μm
Particle loading (ϕ)	0.5
Reynolds number	3.56
Particle Reynolds number	0.089

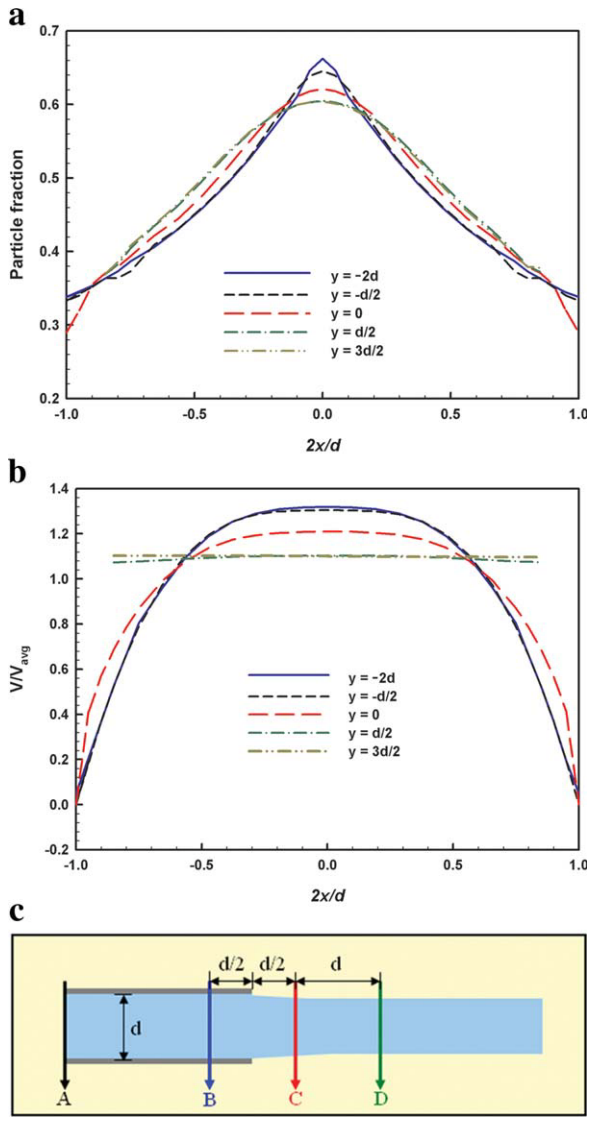

Figure 5. (a) Particle distributions, (b) velocity profiles of the jet flow across the gap or jet at several different positions, the positions are shown at (c).

[Color figure can be viewed in the online issue, which is available at wileyonlinelibrary.com.]

will remain in a nonuniform state considering that the d/a ratio will be very large in most cases.

In Figure 6 we plotted the particle distribution and velocity profiles along the center line for three different particle sizes of $a/d = 0.05$, 0.025 and 0.005. It is noted that as the particle size becomes smaller, the particle fraction at the centerline does not change much from the upstream value. This is a consequence of the scaling law of the diffusivity with particle size. Since the particle diffusivity scales as $\dot{\gamma}a^2$ (Leighton and Acrivos[1]), the migration of 50 μm particles is much smaller than that of 200 μm particles. The velocity profiles converge to their fully developed values within two gap distances, showing slightly faster merge for smaller particles. The fully developed velocity of the smallest particle is the largest. This means that the thickness of the jet is the smallest of all. The problem of die swell will be considered later in more detail. Next we varied the particle loading. In Figure 7 we showed the particle concentration and velocity profiles along the centerline. It is noted that the particle concentration and velocity profiles reach the fully developed state faster as the particle loading increases. The primary reason for the faster development in the suspension with higher loading appears to be the consequences of the increased viscosity. Since the viscosity of the suspension increases with particle loading the momentum diffusion time that is proportional to $d^2/(\eta/\rho)$ decreases with particle loading. Then the developing length becomes shorter with increasing particle loading. This argument can be confirmed when we plot the y-component velocity along the centerline for the Newtonian fluids with the same viscosities as the corresponding suspensions as shown in Figure 7c. The transition length becomes shorter as viscosity increases. However, since the jet thicknesses are not the same due to the inertial effect the scaling law cannot be tested rigorously even in the case of Newtonian fluids. The differences in the transition characteristics among different particles loadings are not as conspicuous as in the Newtonian cases. In the case of suspensions the migration problem should affect the transition

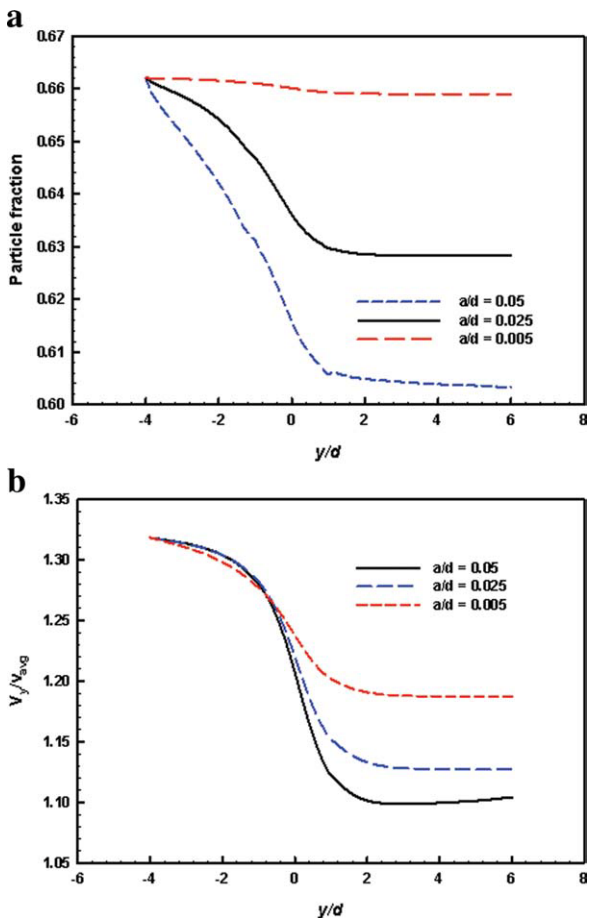

Figure 6. Changes in (a) particle fraction, and (b) y-component velocity at the center of the gap or jet for different particle sizes.

[Color figure can be viewed in the online issue, which is available at wileyonlinelibrary.com.]

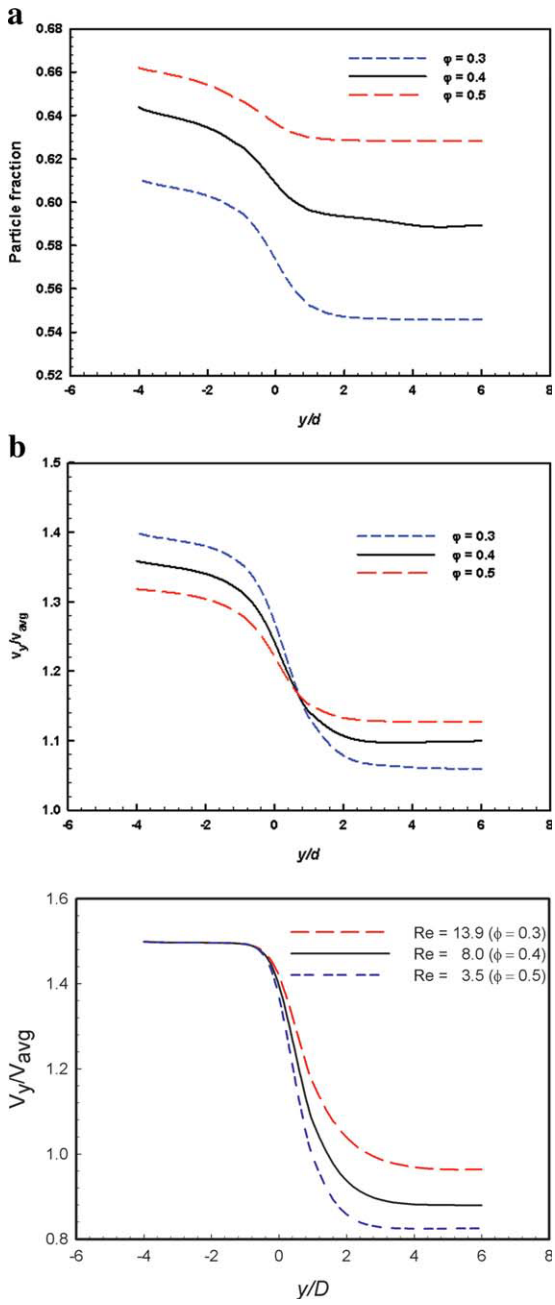

Figure 7. Changes in (a) particle fraction, (b) *y*-component velocity at the center of the gap or jet for different particle loadings, and (c) *y*-component velocity at the center of the gap or jet for Newtonian fluids with the same viscosity as the suspension.

[Color figure can be viewed in the online issue, which is available at wileyonlinelibrary.com.]

length. Since the particle diffusivity is an increasing function of particle concentration in the Phillips et al.'s model, the particles rearrange themselves faster in more concentrated suspension as can be noticed in Figure 7. It appears that in the case of the lower particle loading system the slower rearrangement of particles tends to retard the development of the velocity profiles, and, hence, the difference among different particle loading becomes smaller. We also performed simulations for different particle Reynolds numbers as shown in Figure 8. Inside the gap almost no difference is observed for three different levels of particle Reynolds number studied here, meaning that particle Reynolds number is sufficiently small to neglect the inertial effect, and, hence, the underlying assumption of zero Reynolds number in the Phillips et al.'s model is not violated even though computations were done at finite Re_p. Here the particle Reynolds number Re_p, is defined based on the diameter of particle and the average velocity of suspension ($Re_p = 2au\rho/\eta(\phi_{avg})$). However, outside of the gap there appear slight differences for different particle Reynolds numbers. This is caused by the inertial effect of the macroscopic flow. The inertial effect of the macroscopic flow will be discussed in the later part. The Reynolds number based on the gap distance can be obtained by multiplying the particle Reynolds number by the factor of 20 in this case considering the sizes of the gap and particle. Since the geometry of the system and the material parameters are fixed, the different Reynolds numbers represent the different velocity in this case. Considering the fact that the hydrodynamic diffusivity scales as $\dot{\gamma}a^2$, and the time to travel a fixed distance is inversely proportional to the velocity, hence $\dot{\gamma}$, we can deduce that the diffusion length that is proportional to $\sqrt{D_{hydrodynamic}t}$ is independent of shear rate or

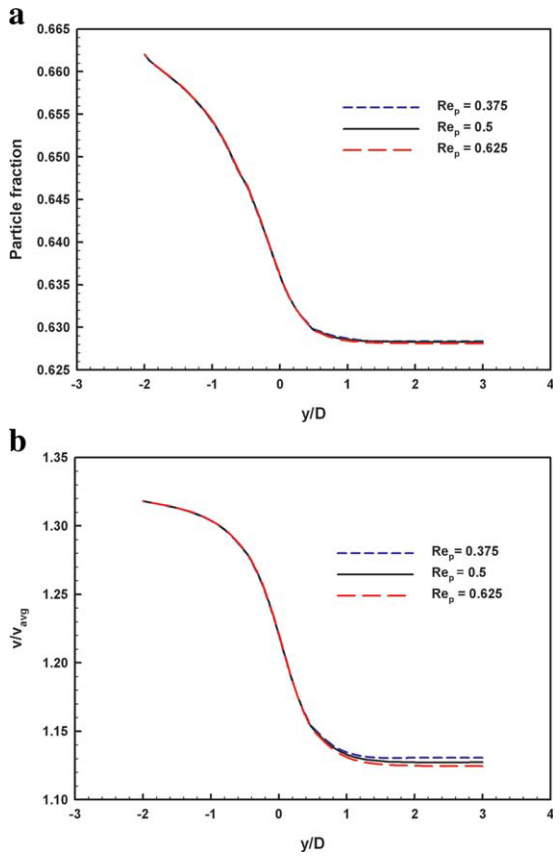

Figure 8. Changes in (a) particle fraction, and (b) *y*-component velocity at the center of the gap or jet for different particle Reynolds number.

[Color figure can be viewed in the online issue, which is available at wileyonlinelibrary.com.]

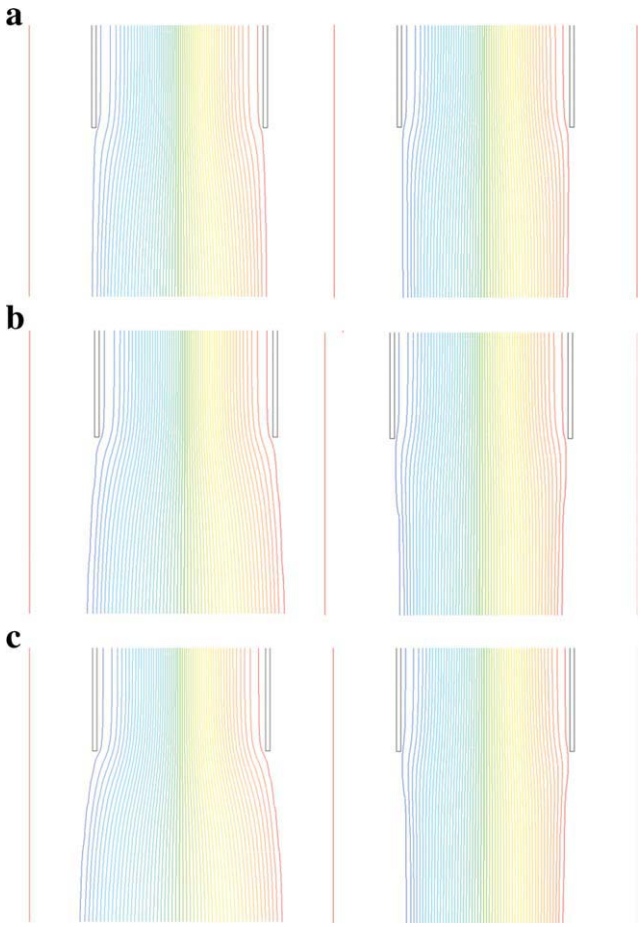

Figure 9. Streamlines of the flow of Newtonian fluid (left) and suspension (right) for different particle loadings of (a) 0.3, (b) 0.4, and (c) 0.5.

The viscosities of Newtonian fluids have the same viscosity as the suspension. The Reynolds numbers based on the gap thickness are (a) 13.9; (b) 8.0; (c) 3.5. [Color figure can be viewed in the online issue, which is available at wileyonline library.com.]

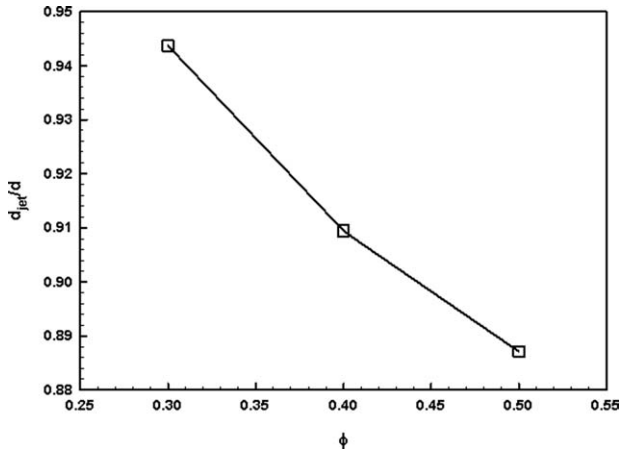

Figure 10. The effect of particle loading on the jet thickness at the fully developed state.

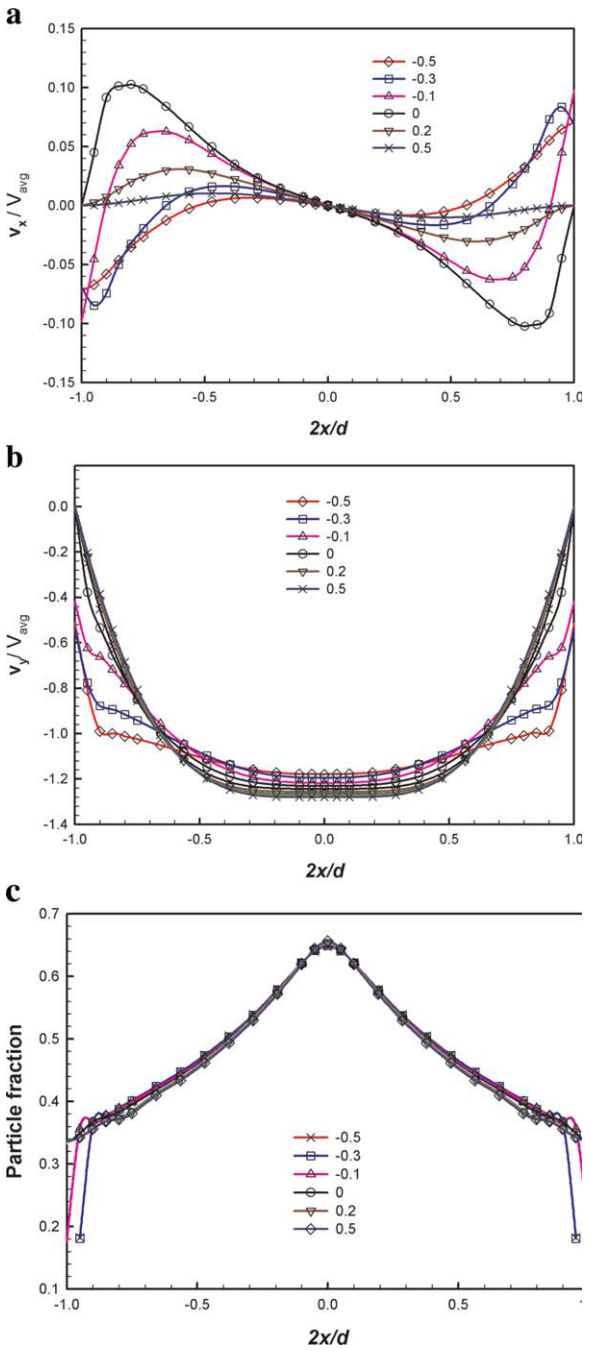

Figure 11. *x*- (a), *y*- (b) component velocity and particle fraction, and (c) profiles near the exit.

[Color figure can be viewed in the online issue, which is available at wileyonlinelibrary.com.]

the average velocity. In other words two opposing effects of the increased hydrodynamic diffusivity due to the increase in the shear rate, and the decreased diffusion time due to faster velocity cancel each other. This means that the particle migration in Newtonian fluid is dependent only on the total shear, which was also observed experimentally for the case of Couette flow.[28]

In Figure 9, we plotted the shapes of the jets for different particle loadings and the die swell behavior of Newtonian

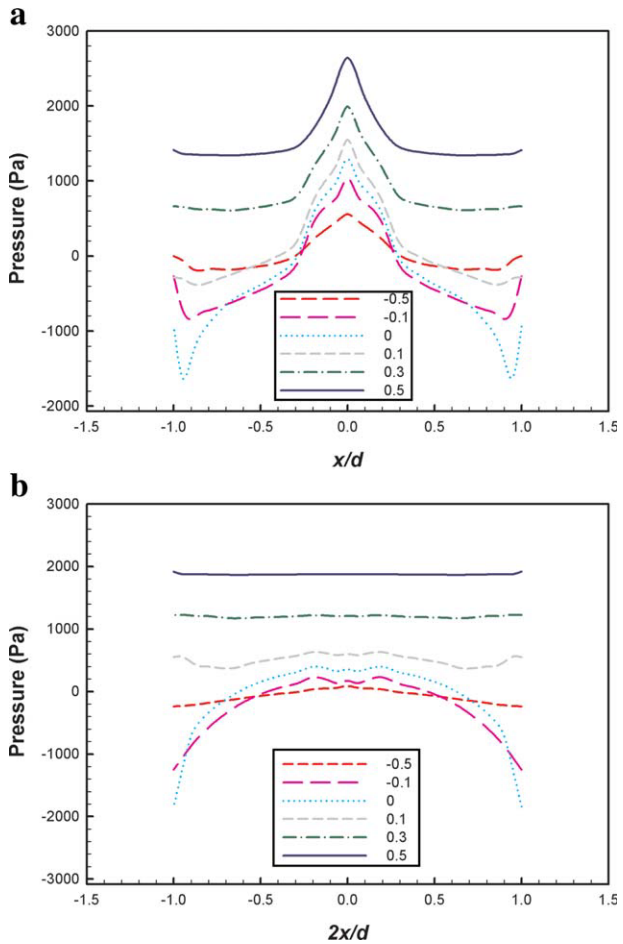

Figure 12. Pressure profiles near the exit for the suspension of ϕ = 0.5 (a), and Newtonian fluid with the same viscosity as the suspension (b).

The Reynolds number is 3.5. The numbers in the legend represent y/d. [Color figure can be viewed in the online issue, which is available at wileyonlinelibrary.com.]

fluids that has the same viscosity as the corresponding suspension. It is noted that the fully developed jet thickness is almost the same as the die gap when $\phi = 0.3$, while it is smaller than the die gap when $\phi = 0.5$. In other words there is die contraction rather than die swell which is observed for the case of Newtonian and polymeric fluids. In Figure 10 we have plotted the jet thicknesses for three different particle loadings. Within the particle loadings tested here the die contraction becomes more conspicuous for larger particle loading. The die swell problem of elastic liquids has been a benchmark problem of the numerical solutions for many years.[29–36] However, the die swell problem of particle laden fluids has not been studied theoretically or numerically. In the case of polymeric liquids the die swell is known to be correlated with the first normal stress difference.[37] For the polymeric fluids the first normal stress difference is positive, and the jet swells as it comes out of the channel. In the case of the circular jet of Newtonian fluids it has been known that there is a 13% increase in the jet diameter when the inertial effect is negligibly small. Zarraga et al.[38] reported that the first normal stress difference of homogeneous suspension of spherical particles in Newtonian fluid is negative and proportional to the shear rate. Therefore, the die contraction is predicted for the suspension if the Miller and Morris' approach[15] was used. However, in this research, the first normal stress difference is zero because we used the Newtonian model with a particle concentration dependent viscosity. Therefore, die contraction observed in this research should be caused by another mechanism explained as follows: Since particles are concentrated at the center of the channel in this study and the wall layers are depleted of particles, velocity blunting results in and the average velocity of the wall layer is much smaller than the core velocity. Here we note that the average wall layer velocity is smaller for the particle loaded system than for the Newtonian case due to the velocity blunting because the core moves as a plug. In Figure 11 the changes in particle concentration and velocity profiles before and after exiting are shown for comparison when particle loading is 0.5. As the suspension flows out of the channel the flow direction velocity of the almost particle free-wall layer catches up the core velocity, and the transverse direction velocity becomes large near the free surface (See Figure 11a and b). In other words, to match the material balance (the equation of continuity), as the interface velocity becomes to the core velocity, the area should be contracted accordingly. This results in the die contraction. During this process there is an abrupt change in the velocity, and, hence, the shear rate of the free surface layer is very large. To keep the free surface stress free there develops a strong nonhomogeneity in shear field. This can be seen in Figure 11a and b. The large shear rate homogeneity induces a strong migration of particles to the core direction to results in the very low-particle concentration at the free-surface region (See Figure 11c). In other words the particle migration toward the center near the free surface is accelerated as the suspension comes out of the die. This mechanism of die contraction can be seen more clearly in Figure 9 where the distance between the two neighboring streamlines adjacent to the wall shrinks abruptly as the suspension comes out of the die exit, while the distances near the center are much the same. In Figure 12 we have plotted the pressure profiles across the gap or jet for Newtonian and particle laden cases. In the case of Newtonian fluid the pressure at the free surface is smaller than the pressure inside the jet. Therefore, the jet swells. In the case of suspension the sign of the pressure gradient reverses at the free surface and the gradient is the largest just at the exit. The pressure field pushes the free surface to the center.

Table 2. Numerical Parameters for the Slot Coating Flow Calculations

Gap size of the slot (d)	0.3 mm
Gap size of the coating bead (h)	0.19 mm
Average inlet velocity	0.2 m/s
Contact angle	20°
Surface tension (σ)	0.05 N/m
Liquid viscosity	0.05 Pa.s
Liquid density	1000 kg/m^3
Particle size (a)	20 μm
Particle loading (ϕ)	0.4
Web speed (v_w)	0.36 m/s
Reynolds number at the die	0.24
Particle Reynolds number at the die	0.032

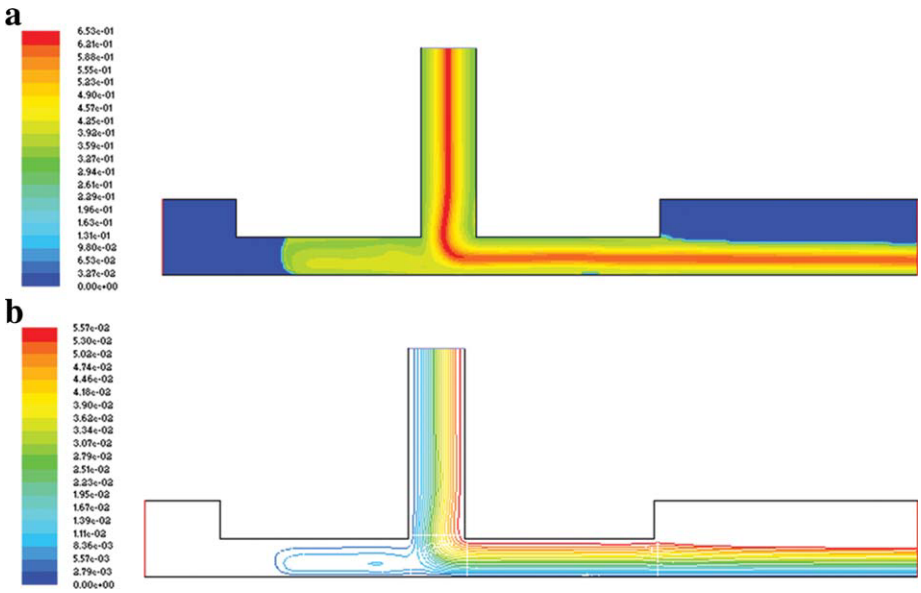

Figure 13. (a) Particle distribution map, and (b) streamlines of the slot coating flow.

[Color figure can be viewed in the online issue, which is available at wileyonlinelibrary.com.]

This results in the die contraction. The reversal of pressure gradient at the jet surface appears to be the consequence of the fulfillment of material balance as described. The uneven distribution of pressure across the gap or the jet appears to be caused by the change in the viscous stress term from the fully developed profile inside the gap where the x-component velocity vanishes. Since the viscosity at the center is large (The particle concentration is close to the maximum packing fraction) a slightly changed velocity profile from the fully developed profile results in the large change in the viscous stress.

Experimentally, as far as the authors are aware of, there has been no report in the literature on the die contraction of suspensions in Newtonian fluid under the creeping flow condition. Furbank and Morris[10] and Nicolas[39] observed die contraction in the jetting of suspension into air. However, in their studies there was a gravity effect while there is no gravity in our system. What gravity does is to pull the jet to have a strong inertial effect. When the inertia is dominant it is known that the die contraction occurs and the ratio is 0.87.[40] Therefore, we cannot be sure whether the die contractions they observed were caused by the same mechanism. Recently Larsen and Shapley[41] observed a die-swell-like flow of suspension in a microfluidic system. However, their system is not the same as ours in that in this research, the flow is strictly 2-D, and the contraction occurs in the gap direction while, in Larsen and Shapley's case, the swell occurs in the span direction while filling the gap that is fixed by solid walls.

Slot Coating Flow

Next we consider the slot coating system as shown in Figure 1b. The numerical parameters chosen here are listed in Table 2. The numerical parameters are typical values for the coating of electrodes in the lithium ion batteries. As was described before, in this case, the thickness and velocity of the suspension at the fully developed downstream are known *a priori*. Considering that the flow inside the coating bead is almost a simple Couette flow, and velocity gradient should vanish in the fully developed flow regime, one may think that there is no mechanism for particle migration in the case of slot coating system. In fact the flow within the coating bead (the region between the die exit and the web) is not trivial. Rather depending on the size of the gap thickness and the bead length, the flow pattern changes. The flow pattern and the particle distribution at the coating bead are not just the extensions of those in the slit die. The reason is that there should be a change in velocity field from a parabolic profile to a flat profile even in the case of purely Newtonian fluid. In the case of suspension the change should be different from the Newtonian case. In Figure 13 we show the particle concentration map at the steady state. In this case the upstream meniscus of the coating bead is located more than three gaps away from the slot exit and the upstream region has a much lower particle concentration than the maximum packing fraction, because the centerline part of the flow inside the slot is convected to the downstream region of the coating bead. The velocity profile is far from being linear inside the coating bead, and due to the uneven distribution of particles the velocity gradients near the two walls are larger than the core of the channel. Since the length of the coating bead is not sufficiently long the particle distribution leaving the downstream of the coating bead is not uniform and close to the particle distribution inside the slot. After exiting the coating bead the velocity profile becomes flat in six times the gap size as shown in Figure 14. Since there is no shear after the flat velocity profile is attained, the particle distribution becomes frozen and the fully developed profile of the particle distribution has the nonuniform distribution. The time t for achieving the flat velocity profile as the suspension comes out of the coating bead scales as h^2/v, where h is the bead thickness, and v is the kinematic viscosity of

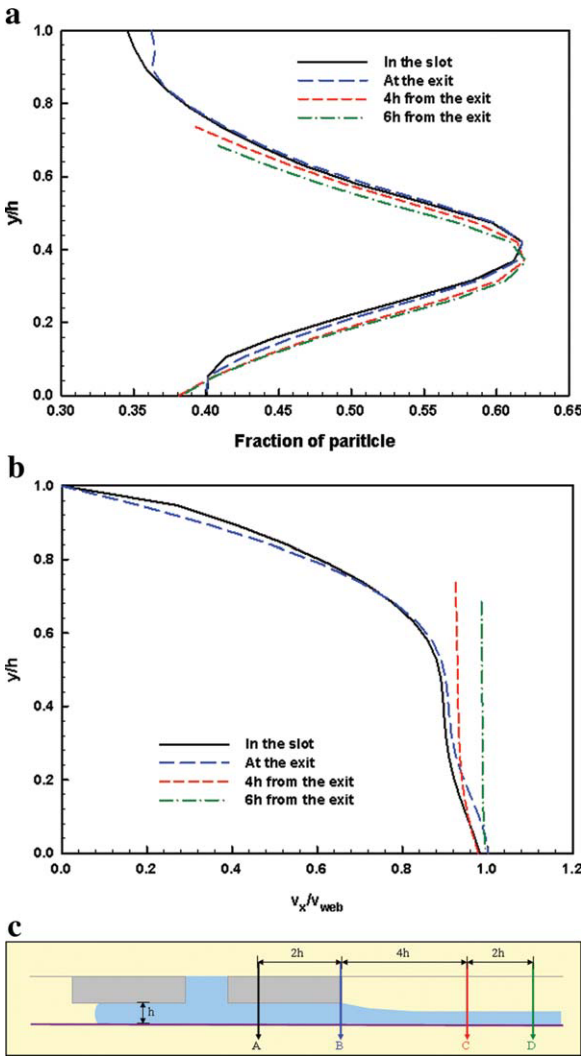

Figure 14. (a) Particle distributions, and (b) velocity profiles at several different positions shown in (c) of the coating flow.

[Color figure can be viewed in the online issue, which is available at wileyonlinelibrary.com.]

the suspension. This means the length L to travel for fluids with the web velocity v_w is $v_w\, t = v_w\, h^2/v$. If we substitute the numerical value given in Table 2 the value of L becomes 0.27 h, which is an order of magnitude shorter than the numerical result of 6 h as described. It should be due to the uneven distribution of particles. Any deeper analysis will require parametric studies while varying relevant parameters. Since it takes a formidably long computation time (About two weeks to one month per each set with a 1.3 GHz Dual-Core CPU/4GB RAM Computer), we did not perform the parametric study for the coating problem as in the case of free-jet problem. We believe the parametric study should be done as a separate project using a parallel computing technique. However, the result presented here bears the most important feature of the particle migration problem. From the result one can see that the length of the slot from the suspension reservoir should be as short as possible to have a more uniform distribution of particles by avoiding the nonuniformity at the inlet to the slot.

Discussion

In this research, we have investigated a planar jet flow and a slot coating flow as the first step toward the understanding of the particle migration with free surfaces. The result shows that, in the jet flow, even though the velocity profile is fully developed and becomes flat the particle distribution never reaches the uniform distribution. The slot coating system shows the similar result on the distribution of particles at the downstream. These results can be valuable information in the design of suspension handling systems such as slot coating or curtain coating, as well as the extrusion of particle laden fluids.

The mathematical model considered here is a macroscopic one, and, hence, the microscopic nature of the system cannot be predicted with this model. There is a possibility of surface deformation due to the motion of particles near the surface as experimentally observed.[6–8] Also there can be the depletion of particles near the surface due to the finiteness of those particles. In their cases there are continuous supplies of the kinetic energy by the motion of belt or gravity which can disturb the surface. However, in these cases of the jet flow and coating flow, solid-like flows are evolved at the downstream, and, therefore, no such visibly large disturbance in surface is expected and the physics of the problem will not be appreciably changed by the possibly present surface change just after the exit from the parallel plates or coating die.

Considering the Miller and Morris model,[16] one may think that the negative N_1 is responsible for the die contraction. According this numerical simulations with the Newtonian model with ϕ-dependent viscosity the die contraction occurs without the effect of N_1. This means that the die swell or contraction of "real" Newtonian suspension with the negative normal stress difference is the combined result of Newtonian die swell, first normal stress difference and the change in the velocity field due to particle migration. The relative importance of each term will determine the magnitude of die swell or contraction.

Acknowledgments

The authors wish to acknowledge the financial support from the Applied Rheology Center, Korea University (ERC supported by Korea Science and Engineering Foundation) through Project Number R112000080500102008.

Literature Cited

1. Leighton D, Acrivos A. The shear induced migration of particles in concentrated suspension. *J Fluid Mech.* 1987;181:415–439.
2. Husband DM, Mondy LA, Ganani E, Graham AL. Direct measurements of shear-induced particle migration in suspensions of bimodal spheres. *Rheol Acta.* 1994;33:185–192.
3. Tirumkuludu M, Tripathi A, Acrivos A. Particle segregation in monodisperse sheared suspension. *Phys Fluids.* 1999;11:507–509.
4. Tirumkuludu M, Mileo A, Acrivos A. Particle segregation in monodisperse sheared suspension in partially filled rotating horizontal cylinder. *Phys Fluids.* 2000;12:1615–1618.

5. Timberlake BD, Morris JF. Concentration band dynamics in free-surface Couette flow of a suspension. *Phys Fluids*. 2002;14:1580–1589.
6. Timberlake BD, Morris JF. Particle migration and free-surface topography in inclined plane flow of a suspension. *J Fluid Mech.* 2005;538:309–341.
7. Singh A, Nir A, Semiat R. Free surface flow of concentrated suspension. *Int J Multiphase Flow*. 2006;32:775–790.
8. Loimer T, Nir A, Semiat R. Shear-induced corrugation of free interfaces in concentrated suspensions. *J Non-Newt Fluid Mech*. 2002; 102:115–134.
9. Apostolou K, Hrymak AN. Discrete element simulation of liquid-particle flows. *Comput Chem. Eng*. 2008;32:841–856.
10. Furbank RJ, Morris JF. An experimental study of particle effects on drop formation. *Phys. Fluids*. 2004;16:1777–1790.
11. Thornell G, Klintberg L, Laurell T, Nilsson J, Johansson S. Desktop microfabrication - initial experiments with a piezoceramic. *J Micromech Microeng*. 1999;9:434–437.
12. Phillips RJ, Armstrong RC, Brown RA, Graham Al, Abbott JR. A constitutive equation for concentrated suspensions that accounts for shear-induced particle migration. *Phys Fluids A*. 1992;4:30–40.
13. Jenkins JT, McTigue DF. *Transport processes in concentrated suspensions: the role of particle fluctuations*. In: Joseph DD, Schaeffer DG, eds. *Two Phase Flows and Waves*. Springer; 1990.
14. Nott PR, Brady JF. Pressure-driven flow of suspensions - Simulations and theory. *J. Fluid Mech.* 1994;275:157–199.
15. Morris JF, Boulay F. Curvilinear flows of noncolloidal suspensions: The role of normal stresses. *J Rheol*. 1999;43:1213–1237
16. Miller RM, Morris JF. Normal stress-driven migration and axial development in pressure-driven flow of concentrated suspensions. *J Non-Newt Fluid Mech.* 2006;135:149–165.
17. Subia SR, Ingber MS, Mondy LA, Altobelli SA, Graham AL. Modelling of concentrated suspensions using a continuum constitutive equation. *J Fluid Mech*. 1998;373:193–219.
18. Kim,JM, Lee SG, Kim C. Numerical simulations of particle migration in suspension flows: Frame-invariant formulation of curvature-induced migration. *J Non-Newt. Fluid Mech*. 2008;150:162–176.
19. Krishnan GP, Beimfohr S. Leighton DT. Shear-induced radial segregation in bidisperse suspensions. *J Fluid Mech.* 1996;321:371–393.
20. Shapley NC, Brown RA, Armstrong RC. Evaluation of particle migration models based on laser Doppler velocimetry measurements in concentrated suspensions. *J Rheol*. 2004;48:255–279.
21. Lyon MK, Leal LG. An experimental study of the motion of concentrated suspensions in two-directional channel flow. Part 1. Monodisperse systems. *J Fluid Mech*. 1998;363:25–56.
22. Fang Z, Phan-Thien N. Numerical simulation of particle migration in concentrated suspensions by a finite volume method. *J Non-Newt Fluid Mech.* 1995;58:67–81.
23. Kim C. Mathematical model of migration of spherical particles in tube flow under the influence of inertia and particle-particle interaction. *Korean J Chem Eng*. 2004;21:27–33.
24. Zhang K, Acrivos A. Viscous resuspension in fully developed laminar pipe flows. *Int J Multiphase flow*. 1994;20:579–591.
25. Koh CJ, Hookam P, Leal LG. An experimental investigation of concentrated uspension flows in a rectangular channel. *J Fluid Mech*. 1994;266:1–32.
26. Han MS, Kim C, Kim M, Lee S. Particle migration in tube flow of suspensions. *J Rheol*. 1999;43:1157–1174.
27. Andre P, Clermont JR. Numerical simulation of the die swell problem of a Newtonain fluid by using the concept of stream function and a local analysis of the singularity at the corner. *J Non-Newt Fluid Mech*. 1987;23:335–354.
28. Abbott JR, Tetlow N, Graham AL, Altobelli SA, Fukushima E, Mondy LA, Stephens TS. Experimental observations of particle migration in concentrated suspensions: Couette flow. *J Rheol*. 1994; 35:773–795.
29. Crochet MJ, Keunings R. Die swell of a maxwell fluid -Numerical Prediction. *J Non-Newt Fluid Mech*. 1980;7:199–212.
30. Crochet MJ, Keunings R. On numerical die swell calculation. *J Non-Newt Fluid Mech*. 1982;10:85–94.
31. Ahn YC, Ryan ME. A finite difference analysis of extrudate swell problem. *Int J Num Methods Fluids*. 1991;13:1289–1310.
32. Clermont JR, Normandin M. Numerical simulation of extrudate swell for Oldroyd-B Fluids using the stream tube analysis and streamline approximation. *J Non-Newt Fluid Mech*. 1993;50:193–215.
33. Ahmed R, Liang RF, Mackley MR. The experimental-observation and numerical prediction of planar entry flow and diw swell for molten polyethylenes. *J Non-Newt. Fluid Mech* 1995;59:129–153.
34. Ngamaramvaranggul V, Webster MF. Viscoelastic simulations of stick-slip and die swell flows. *Int. J. Num. Methods Fluids*. 2001;36: 539–595.
35. Tome MF, Mangiavacchi N, Cuminato JA, Castello A, McKee S. A finite difference technique for simulating unsteady viscoelastic free surface flows. *J Non-Newt Fluid Mech*. 2002;106:61–106.
36. Tome MF, Grossi L, Castelo A, Cuminato JA, McKee S, Walters K. Die swell, splashing drop and a numerical technique for solving the Oldroyd B model for axisymmetric free surface flows. *J Non-Newt Fluid Mech*. 2007;141:148–166.
37. Tanner RI. *Engineering Rheology*. New York, Oxford Univsersity Press; 1985.
38. Zarraga IE, Hill DA, Leighton DT. The characterization of the total stress of concentrated suspensions of noncolloidal spheres in Newtonian fluids. *J Rheol*. 2000;44:185–220.
39. Nicolas M. Experimental study of gravity-driven dense suspension jets. *Phys Fluids*. 2002;14:3570–3576.
40. Denn MM. *Process Fluid Mechanics*. Englewood Cliffs, Prentice Hall, 1980.
41. Larsen MU, Shapley N. Multilayer microfluidic flows of suspensions and flow focusing. Presented at the 79th Annual Meeting of the Society of Rheology; Oct 7–11, 2007; Salt Lake City, UT.

Manuscript received Mar. 27, 2009, revision received Sept. 15, 2009, and final revision received Dec. 1, 2009.